ACTA
PROTOZOOLOGICA

Acta Protozool. (2015) 54: 123–135
www.ejournals.eu/Acta-Protozoologica
doi:10.4467/16890027AP.15.010.2735

Morphology, Ciliary Pattern and Molecular Phylogeny of *Trachelophyllum brachypharynx* Levander, 1894 (Litostomatea, Haptoria, Spathidiida)

Seok Won JANG[1]*, Peter VĎAČNÝ[2]*, Shahed Uddin Ahmed SHAZIB[1] and Mann Kyoon SHIN[1]

[1]University of Ulsan, Department of Biological Science, Ulsan, South Korea; [2]Comenius University, Department of Zoology, Bratislava, Slovakia; *Co-first authors

Abstract. We isolated a relatively unknown haptorian ciliate, *Trachelophyllum brachypharynx*, in brackish water from the mouth of the Taehwa River, South Korea. The morphology of this isolate was studied using *in vivo* observation and protargol impregnation, and its evolutionary history was revealed by phylogenetic analysis of the 18S rRNA gene. The main features of *T. brachypharynx* include (i) a very narrowly fusiform and slightly contractile body about 380 × 40 μm in size; (ii) two ellipsoidal macronuclear nodules typically connected by a fine strand; (iii) a single terminal contractile vacuole; (iv) filiform extrusomes that are typically 30 μm long; (v) an average of 24 ciliary rows, with two of them anteriorly differentiated into an isostichad dikinetidal dorsal brush; and (vi) hat-shaped lepidosomes. Based on the 18S rRNA gene phylogeny, *T. brachypharynx* clustered together with *Trachelophyllum* sp. within the order Spathidiida. Furthermore, phylogenetic trees and networks indicate some members from the genera *Enchelyodon* and *Spathidium* as the nearest relatives of trachelophyllids. Therefore, based on the present molecular and comparative-morphological analyses, we suggested a hypothesis explaining how trachelophyllids may have evolved from a spathidiid-like ancestor via an enchelyodonid-like stage.

Key words: 18S rRNA gene, dorsal brush, Korea, lepidosomes, Trachelophyllidae.

INTRODUCTION

The order Spathidiida Foissner & Foissner, 1988 is a diverse assemblage of holotrichously ciliated haptorians that are typically characterized with bursiform to spatulate bodies, a three-rowed dorsal brush, and anteriorly curved ciliary rows (Foissner and Xu 2007). Recent molecular studies have indicated that trachelophyllids and several "traditional" haptorids belong to this taxonomically difficult group (Vďačný *et al.* 2011, 2012, 2014; Vďačný and Foissner 2013). However, trachelophyllids morphologically deviate from other spathidiids in that (i) their body is covered by a mucilaginous layer of complex organic epicortical scales, called lepidosomes; (ii) their oral ciliature is in an enchelyodonid pattern in that the anterior end of somatic kineties is not curved in oral region; and (iii) the first two brush rows are dikinetidal while the third row is monokinetidal throughout (Foissner 1994, 2005; Foissner *et al.* 1999, 2002). On the contrary, in spathidiids *sensu stricto*, (i) lepidosomes should not be present, (ii) the anterior end of all ciliary rows should

Address for correspondence: Mann Kyoon Shin, Department of Biological Science, College of Natural Sciences, University of Ulsan, Ulsan 680-749, South Korea. E-mail: mkshin@ulsan.ac.kr

curve rightward forming a spathidiid pattern, and (iii) all three brush rows should be made of dikinetids with only the third row continuing as a monokinetidal tail (Foissner and Xu 2007).

The general body organization of all trachelophyllids is very similar at first glance, but modern investigations have shown lepidosome morphologies to be highly diverse and hence taxonomically important. Based on the shape and number of lepidosome types, six trachelophyllid genera are recognized (Foissner 1994, 2005; Foissner *et al*. 2002): *Bilamellophrya* Foissner *et al.*, 2002; *Epitholiolus* Foissner *et al.*, 2002; *Luporinophrys* Foissner, 2005; *Sleighophrys* Foissner, 2005; *Spetazoon* Foissner, 1994; and *Trachelophyllum* Claparède & Lachmann, 1859.

Trachelophyllids prefer terrestrial and semiterrestrial habitats (Kahl 1930; Foissner 1984, 1994, 2005; Foissner *et al.* 2002), but some have also been found in freshwater (Foissner *et al.* 1995, 1999) and one species, *Trachelophyllum brachypharynx* Levander, 1894, was reported from saltwater (e.g., Levander 1894, 1901; Coats and Clamp 2009; Telesh *et al.* 2009). We found a population of this species in brackish water from the mouth of the Taehwa River opening into the East Sea near the town of Ulsan, South Korea. Since its original description 120 years ago, this species has not been studied using modern alpha-taxonomic and molecular methods. Moreover, our molecular and comparative-morphological phylogenetic analyses provide an explanation how the special trachelophyllid cytoarchitecture may have evolved from a spathidiid-like ancestor via an enchelyodonid-like stage.

MATERIALS AND METHODS

Material collecting, processing, and taxonomic methods

Samples containing *T. brachypharynx* were collected on January 23, 2014 from the mouth of the Taehwa River opening into the East Sea near the town of Ulsan, South Korea (129°16′58″E 35°33′9″N). The samples were taken about 1.0 m off shore and consisted of about 0.5 liter of brackish water (8‰ salinity) and some underlying substratum. The collected material was immediately transported to the laboratory where a raw culture was established in a Petri dish with a diameter of 87 mm. No wheat grains or prey organisms were added into the culture. After about one week, a few *T. brachypharynx* specimens appeared in the culture but then disappeared after about seven days.

Living specimens were observed under an optical microscope Axio Imager A1 (Carl Zeiss, Oberkochen, Germany) at low (50–400 ×) and high (1,000 ×; immersion) magnifications using bright field and differential interference contrast optics. Ciliary pattern and nuclear apparatus were revealed by the protargol impregnation method according to Wilbert (1975), and were studied under the optical microscope at high magnification. Measurements of living specimens were performed at magnifications of 40–1,000 ×, while those on impregnated specimens were carried out at a magnification of 1,000 ×. Images were captured using a CCD camera (Axio Cam MRc; Carl Zeiss) and were adjusted using Adobe Photoshop CS5. Drawings are based on the micrographs of free-swimming and protargol-impregnated specimens. Terminology follows that described in Foissner and Xu (2007) and Foissner (2005).

Molecular methods

One or several *T. brachypharynx* specimens were picked from the raw Petri dish culture, washed several times to remove contaminants, and transferred into an 1.5 ml microtube with a minimum volume of sterile water. The other five samples were prepared as described above to test the quality and reliability of the obtained sequences. All samples were processed separately for DNA extraction, PCR amplification and sequencing.

The RED Extract-N-Amp Tissue PCR Kit (Sigma, St. Louis, MO, USA) was used to extract genomic DNA following the manufacturer's instruction, except for reducing the reaction volume to one tenth for single-cell samples and to one fifth for multiple-cell samples. The 18S rRNA gene of *T. brachypharynx* was amplified using the TaKaRa ExTaq DNA polymerase Kit (TaKaRa Biomedicals, Otsu, Japan) and the eukaryotic universal forward EukA (5'-AAC CTG GTT GAT CCT GCC AG-3') and reverse EukB (5'-CAC TTG GAC GTC TTC CTA GT-3') primers (Medlin *et al.* 1988). PCR cycling conditions followed the protocol described in Chen and Song (2001). After PCR, amplified DNA was confirmed by electrophoresis on 1.2% agarose gels. Consequently, PCR products were directly used for sequencing (ABI 3730 automatic sequencer; Macrogen Inc., Seoul, Korea). No polymorphisms were found among *T. brachypharynx* sequences.

Phylogenetic methods

To reveal the phylogenetic position of *T. brachypharynx*, an alignment containing 18S rRNA gene sequences of 69 litostomatean taxa was constructed using MAFFT ver. 7.0 with the Q-INS-I strategy (Katoh and Toh 2008). The alignment was refined according to the column scores calculated in G-blocks ver. 0.91b (Castresana 2000; Talavera and Castresana 2007). GTR + I (= 0.5960) + Γ (= 0.4870) was the best fit evolutionary substitution model found for the alignment using jModelTest ver. 2.0.1 under the Akaike Information Criterion (Guindon and Gascuel 2003; Posada 2008). Bayesian inference was carried out under this model using the computer program MrBayes ver. 3.2.1 (Ronquist and Huelsenbeck 2003), which was run with four MCMC chains (one cold and three heated) for 5,000,000 generations with a sample frequency of 100 generations. The first 25% of sampled trees were discarded as burn-in. The remaining trees were used to construct a 50% majority-rule consensus tree and to calculate branch lengths and posterior probabilities (PP). Maximum likelihood (ML) analyses were carried out using PhyML ver. 3.0 (Guindon *et al.* 2010) under the GTR + I + Γ model and with 1,000 nonparametric bootstrap replicates.

We tested four alternative evolutionary scenarios opposite to the topology in the best unconstrained tree (Table 1). Unconstrained and constrained trees were built in PAUP* ver. 4.0b (Swofford 2003), using the ML criterion, the GTR + I + Γ evolutionary model selected by jModelTest, a heuristic search with TBR branch swapping, and 10 random sequence addition replicates. Log likelihoods of constrained trees were statistically compared to that of the best unconstrained tree, using the approximately unbiased, weighted Shimodaira-Hasegawa and weighted Kishino-Hasegawa tests using CONSEL ver. 0.1j (Shimodaira and Hasegawa 2001; Shimodaira 2002, 2008). A p-value < 0.05 was chosen to reject the null hypothesis that the log likelihoods of the constrained and best unconstrained trees were not significantly different.

To visualize all possible phylogenetic trajectories that could be inferred from the 18S rRNA gene alignment, a phylogenetic network was calculated using the NeighborNet algorithm with uncorrected distances. The reliability of the network was assessed with 1,000 bootstrap replicates generated in SplitsTree ver. 4 (Huson 1998; Huson and Bryant 2006).

RESULTS

Trachelophyllum brachypharynx Levander, 1894

1894 ***Trachelophyllum brachypharynx*** – Levander, *Acta Soc. Fauna Flora fenn.* **12:** 66, Taf. III, Fig. 1 [reproduced here as Fig. 35] (original description).

1930 ***Trachelophyllum brachypharynx*** **Levander, 1894** – Kahl, *Tierwelt Dtl.* **18:** 115, Fig. S. 104, *5* [reproduced here as Fig. 36] (revision).

Improved diagnosis (Korean population): Size about 380 × 40 µm *in vivo*, slightly contractile. Shape very narrowly fusiform, with a slightly to distinctly narrowed neck, gradually merging into a broadened trunk. Two ellipsoidal macronuclear nodules usually connected by a fine strand, with two to three broadly ellipsoidal micronuclei close to or attached to macronuclear nodules. Contractile vacuole terminal and comparatively small. Extrusomes filiform, slightly curved and with pointed ends, 30 µm long *in vivo*. On average, 24 ciliary rows, two anteriorly differentiated into an isostichad dikinetidal dorsal brush: row 1 composed of 40 dikinetids on average, row 2 of 33 dikinetids on average. Lepidosomes hat-shaped and about 4 × 3.7 µm *in vivo*.

Type locality: Levander (1894) discovered *T. brachypharynx* in brackish water from the Finnish shore.

Voucher material: Three slides with protargol-impregnated Korean specimens have been deposited in the Natural Institute of Biological Resources (NIBR), Incheon, South Korea with the following registration numbers NIBRPR0000105674. The relevant specimens are marked with ink circles on the backside of the slides.

Gene sequence: The 18S rRNA gene sequence of the Korean population has been deposited in GenBank with the accession number KJ680555. The sequence is 1543 nucleotides long and has a GC content of 43.1%.

Etymology: Not given in the original description. The name is a composite of the Greek prefix *brachy-*

Table 1. Log likelihoods and p-values of AU (approximately unbiased), WSH (weighted Shimodaira-Hasegawa), and WKH (weighted Kishino-Hasegawa) tests for tree comparisons considering different topological scenarios. Significant differences (p-value < 0.05) between the best unconstrained and constrained topologies are in bold.

Topology	Log likelihood (–ln L)	Δ (–ln L)[a]	AU	WSH	WKH	Conclusion
Best maximum likelihood tree (unconstrained)	10823.3288	–	0.788	0.957	0.733	–
Monophyly of spathidiids with enchelyodonid-like oral ciliary pattern (*Enchelyodon* JF263446 + *Lagynophrya acuminata* + *Trachelophyllum* sp. + *T. brachypharynx*)	10848.0276	24.70	**0.012**	0.051	**0.019**	**Rejected**
Monophyly of *Enchelyodon* and spathidiids with enchelyodonid-like oral ciliary pattern (*Enchelyodon* spp. + *L. acuminata* + *Trachelophyllum* sp. + *T. brachypharynx*)	11051.8316	228.50	**2e–08**	**0.000**	**0.000**	**Rejected**
Monophyly of haptorids and spathidiids with enchelyodonid-like oral ciliary pattern (*Enchelyodon* spp. + *Fuscheria* spp. + *L. acuminata* + *Trachelophyllum* sp. + *T. brachypharynx*)	10873.3366	50.01	**5e–05**	**0.004**	**0.001**	**Rejected**
Monophyly of trachelophyllids and *Spathidium* sp. JF263451 (*Trachelophyllum* sp. + *T. brachypharynx* + *Spathidium* sp. JF263451)[b]	10827.7315	4.40	0.283	0.558	0.267	Not rejected

[a] Difference between log likelihoods of constrained and best (unconstrained) tree.
[b] This relationship was indicated by the phylogenetic network analyses.

(*βραχυ*-; short) and the Latin noun *pharynx*, referring to the short cytopharynx of the species. Because the species epithet stands in apposition to the generic name [Article 11.9.1.2 of ICZN (1999)], its ending need not agree in gender with the generic name with which it is combined and must not be changed to agree in gender with the generic name [Article 34.2.1 of ICZN (1999)].

Description of Korean population: Size *in vivo* about 330–445 × 35–45 µm, usually near 380 × 40 µm; morphometric data from protargol-impregnated specimens indicate shrinkage of body length by about 12% and inflation of body width by about 20% (Table 2). Body flexible, up to 2:1 flattened dorsoventrally, and slightly contractile especially in neck region; both contraction and extension occur slowly, thus exact body shape and size difficult to determine. Shape very narrowly fusiform both *in vivo* and after protargol impregnation, but prepared specimens appear stouter on average due to length shrinkage and width inflation (see above), i.e., body length:width ratio 9.7:1 *in vivo* while

Table 2. Morphometric data on the Korean population of *Trachelophyllum brachypharynx*. CV – coefficient of variation (%), I – *in vivo*, M – median, Max – maximum, Mean – arithmetic mean, Min – minimum, MT – method, n – number of individuals investigated, P – protargol impregnation, SD – standard deviation, SE – standard error of arithmetic mean.

Characteristics	MT	Mean	M	SD	SE	CV	Min	Max	n
Body, length (µm)	I	383.8	375.6	38.0	14.4	9.9	329.9	444.6	7
	P	332.2	334.5	45.8	8.4	13.8	246.4	426.0	30
Body, width (µm)	I	39.7	39.3	3.9	1.5	9.8	35.4	45.3	7
	P	41.8	40.2	10.0	1.8	23.9	26.6	66.3	30
Body, length:width ratio	I	9.7	10.0	1.0	0.4	10.6	7.6	10.7	7
	P	8.3	8.3	2.0	0.4	23.7	4.1	14.1	30
Oral bulge, height (µm)	P	7.0	7.2	1.8	0.4	25.7	4.2	10.7	20
Oral bulge, diameter (µm)	P	7.8	7.5	1.5	0.3	18.6	5.4	11.0	23
Anterior body end to macronucleus, distance (µm)	P	143.4	149.8	33.1	6.8	23.1	74.0	233.6	24
Nuclear figure, length (µm)	P	111.4	105.1	19.1	3.9	17.1	71.5	145.2	24
Anterior macronuclear nodule, length (µm)	I	34.3	35.8	5.8	2.4	17.0	27.4	42.8	6
	P	48.3	46.8	9.5	1.7	19.6	25.8	71.2	32
Anterior macronuclear nodule, width (µm)	I	16.7	16.9	1.5	0.6	8.9	14.5	18.5	6
	P	24.8	23.7	5.9	1.0	23.8	12.5	40.2	32
Posterior macronuclear nodule, length (µm)	I	31.1	32.3	4.5	1.8	14.4	24.7	36.1	6
	P	46.1	44.4	10.3	1.8	22.3	25.1	83.1	32
Posterior macronuclear nodule, width (µm)	I	17.5	18.3	2.4	1.0	13.9	13.4	19.7	6
	P	24.3	23.8	5.5	1.0	22.6	13.1	40.1	32
Macronuclear nodules, distance in between (µm)	P	111.4	105.1	19.1	3.9	17.1	71.5	145.2	24
Macronuclear nodules, number	P	2.0	2.0	0.0	0.0	0.0	2.0	2.0	32
Micronuclei, length (µm)	P	4.2	4.0	0.8	0.2	19.0	3.0	5.8	16
Micronuclei, width (µm)	P	2.8	2.8	0.5	0.1	19.5	1.9	3.5	16
Micronuclei, number	P	1.6	2.0	0.6	0.2	38.1	1.0	3.0	16
Somatic kineties, number	P	23.6	24.0	1.7	0.6	7.3	20.0	25.0	7
Kinetids in a ventral kinety, number	P	122.0	119.0	16.7	9.6	13.7	107.0	140.0	3
Circumoral kinety to last dikinetid of brush row 1, distance (µm)	P	94.8	94.9	15.8	4.6	16.7	72.5	124.0	12
Circumoral kinety to last dikinetid of brush row 2, distance (µm)	P	79.3	80.4	11.0	3.2	13.8	63.0	97.7	12
Dorsal brush 1, number of dikinetids	P	39.6	40.0	1.9	0.6	4.7	36.0	42.0	11
Dorsal brush 2, number of dikinetids	P	32.5	33.0	1.6	0.5	4.8	30.0	35.0	11
Dikinetidal brush rows, number[a]	P	2.0	2.0	0.0	0.0	0.0	2.0	2.0	12

[a] One malformed specimen had three dikinetidal brush rows.

8.3:1 after protargol impregnation. Anterior end rather conspicuous due to pin-shaped to conical oral bulge and slightly broadened neck region below it, forming a head-like structure (Figs 2–4, 22, 24). Neck distinctly narrowed and usually slightly curved in extended specimens, while more or less inconspicuous in contracted ones; gradually merges into broadened trunk. Posterior body end typically narrowly rounded, sometimes pointed (Figs 1, 5, 13–21, 27, 29, 30).

Nuclear apparatus in middle trunk region; typically composed of two macronuclear nodules and several micronuclei. Macronuclear nodules broadly to narrowly ellipsoidal, on average ellipsoidal, with a length width ratio of 1.3–3.6:1, with an average near 2:1 both *in vivo* and after protargol impregnation; size about 32 × 17 µm *in vivo*, while 48 × 25 µm after impregnation; usually distinctly apart and connected by a fine strand, very rarely abutting (in one out of 30 specimens analyzed). Nucleoli numerous, small to medium-sized, rounded to narrowly ellipsoidal, evenly distributed over macronuclear nodules, well recognizable after protargol impregnation. Two to three micronuclei attached to macronuclear nodules at varying positions, rarely slightly distant from them, broadly ellipsoidal, i.e., approximately 4 × 3 µm in size after protargol impregnation (Table 2; Figs 1, 5, 14–20, 26–28, 30).

Contractile vacuole in rear end, comparatively small with respect to body size, i.e., about 14 µm across during diastole; sometimes a defecation vacuole near by (Figs 1, 13–17, 19, 20, 27, 29, 30). Extrusomes about 30 × 0.7 µm long in vivo, filiform with pointed and slightly curved ends, attached to oral bulge and scattered throughout cytoplasm, usually heavily impregnated with the protargol method used, rarely with small darker granules in weakly impregnated specimens (Figs 5, 8, 9, 11, 22, 23, 25). Cortex about 1 µm thick and flexible, without granules, covered by mucilaginous layer difficult to recognize *in vivo* and almost indistinguishable in protargol preparations; lepidosomes hat-shaped and about 4 × 3.7 µm in size (Figs 10, 29), no other lepidosome types were recognized due to the lack of SEM observations. Cytoplasm colourless, usually turbid, packed with lipid droplets about 1–10 µm in diameter (Figs 21, 27, 28). The organism glides slowly on the surface of microscope slide and swims by rotation about the main body axis.

Cilia about 13 µm long *in vivo*; arranged in an average of 24 meridional, equidistantly spaced rows; anterior end of somatic kineties not curved in oral region and thus forming an enchelyodonid pattern; some rows shortened anteriorly or posteriorly (Table 2; Fig. 5). Dorsal brush three-rowed and isostichad, i.e., row length difference < 30%. Brush rows 1 and 2 dikinetidal; about 95 µm and 80 µm long, respectively, after protargol impregnation; composed of an average of 40 and 33 dikinetids, respectively; dikinetids more densely spaced in anterior brush portion than in posterior portion; associated with 5 µm long, slightly inflated bristles becoming rod-like in protargol preparations. Brush row 3 monokinetidal throughout, bearing about 1 µm long stumps; with a short anterior dikinetidal tail in a single malformed specimen (Table 2; Figs 6, 7, 12, 31, 32).

Oral bulge rather conspicuous because distinctly set off from body proper; pin-shaped in extended specimens, while conical in contracted cells; not covered by lepidosomes (Figs 2–4, 11, 21, 22, 24, 27, 28, 30). Pharyngeal basket not recognizable *in vivo* and in protargol preparations. Circumoral kinety at base of oral bulge, composed of comparatively widely spaced, more or less oblique dikinetids situated on top of somatic ciliary rows (Figs 6, 7, 25, 32).

Molecular phylogeny of *T. brachypharynx*

In the Bayesian tree, *T. brachypharynx* was placed within the paraphyletic order Spathidiida; however, the statistical support for this placement was insignificant (0.51 PP; Fig. 33). This node was not recognized in the ML analyses that showed the order Spathidiida as polyphyletic. On the other hand, monophyly of the order Spathidiida was sustained by relatively long parallel edges and 69% bootstrap support (BS) in the phylogenetic network. In both Bayesian and ML analyses, *T. brachypharynx* clustered with *Trachelophyllum* sp. with strong statistical support (1.00 PP, 98% ML). Likewise, these two taxa formed a fully supported (100% BS), comparatively long split in the network analyses. Tree-building methods consistently indicated a sister relationship between the trachelophyllids and *Enchelyodon* sp. JF263446, but with very poor statistical support (0.89 PP, 36% ML). Phylogenetic network analyses suggested *Spathidium* sp. JF263451 as a nearest relative of the trachelophyllids; however, this was with a bootstrap support of only 34%. A cluster of trachelophyllids, *Enchelyodon* sp. JF263446, and *Spathidium* sp. JF263451 received a bootstrap support of 51% in the NeighborNet graph.

A monophyletic origin of the spathidiids with an enchelyodonid oral ciliary pattern (i.e., ciliary rows extend meridionally throughout and thus do not curve anteriorly) was rejected by the AU and WKH topology

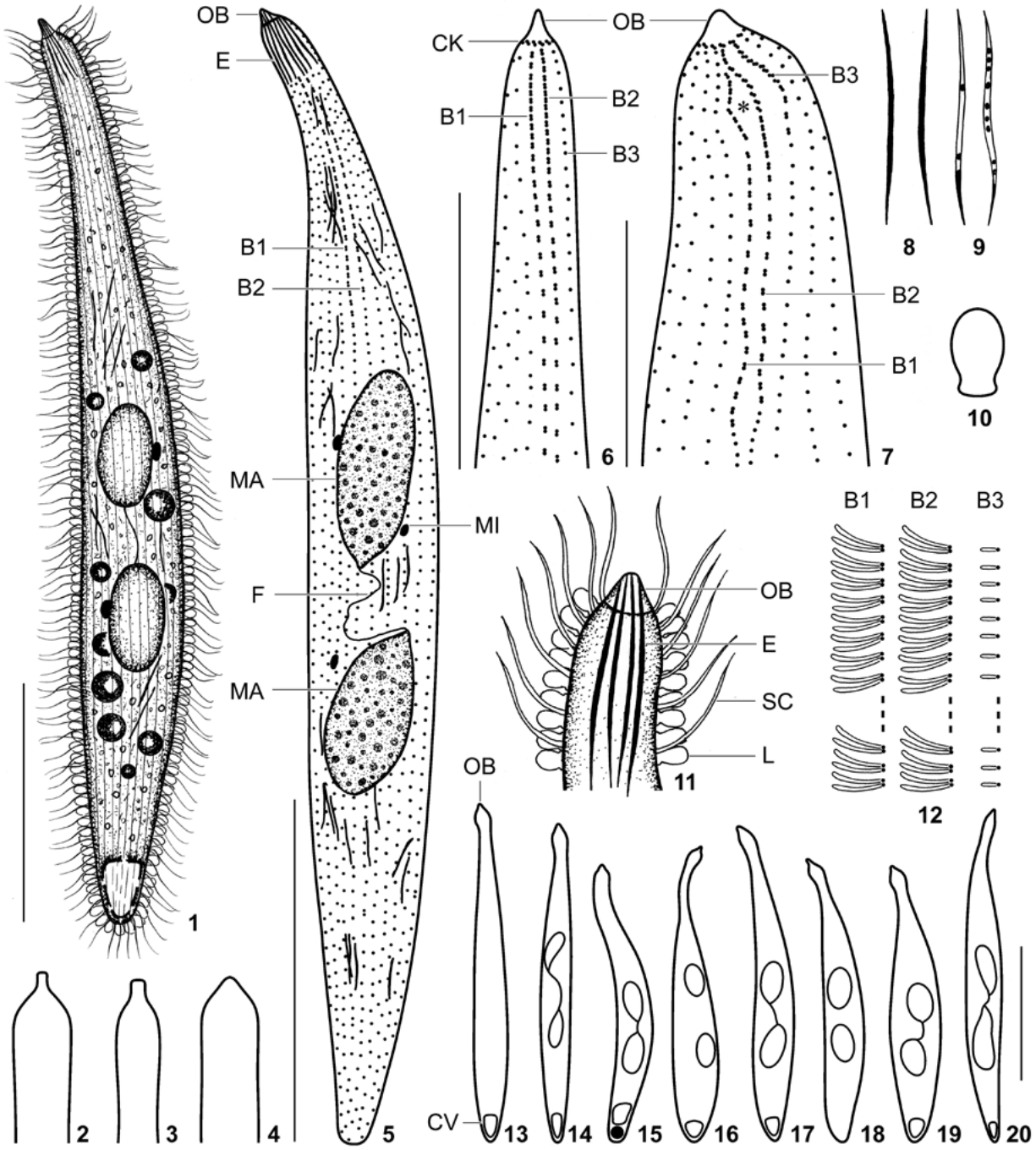

Figs 1–20. *Trachelophyllum brachypharynx*, Korean specimens *in vivo* (1–4, 8, 10–16) and after protargol impregnation (5–7, 9, 17–20). **1** – ventral view of a representative specimen; **2–4** – the pin-shaped oral bulge becomes conical in contracted specimens; **5** – ventral view of the ciliary pattern and nuclear apparatus of a typical specimen; **6, 7** – dorsal view of the ciliary pattern in the anterior body portion of a normal (6) and abnormal (7) specimen. Typically, only brush row 1 and 2 are composed of dikinetids, while brush row 3 is monokinetidal throughout. In the abnormal specimen, brush row 3 also commences with a dikinetidal part but the brush is deformed (asterisk); **8, 9** – extrusomes are about 30 µm long *in vivo* and are filiform with pointed and slightly curved ends (8). When weakly impregnated, they display some small darker granules; **10** – lepidosomes are hat-shaped and about 4 × 3.7 µm in size; **11** – detail of the anterior body portion showing the conical oral bulge, the long filiform extrusomes, and the hat-shaped lepidosomes; **12** – the dorsal brush consists of three-rows. The first two rows are dikinetidal and bear 5 µm long, slightly inflated bristles, while the third row is monokinetidal and associated with 1 µm long stumps; **13–20** – variability in body shape and size as well as nuclear apparatus. Drawn to scale. B1–3 – dorsal brush row 1–3, CK – circumoral kinety, CV – contractile vacuole, E – extrusomes, F – fiber, L – lepidosomes, MA – macronuclear nodules, MI – micronucleus, OB – oral bulge, SC – somatic cilia. Scale bars: 50 µm (6, 7) and 100 µm (1, 5, 13–20).

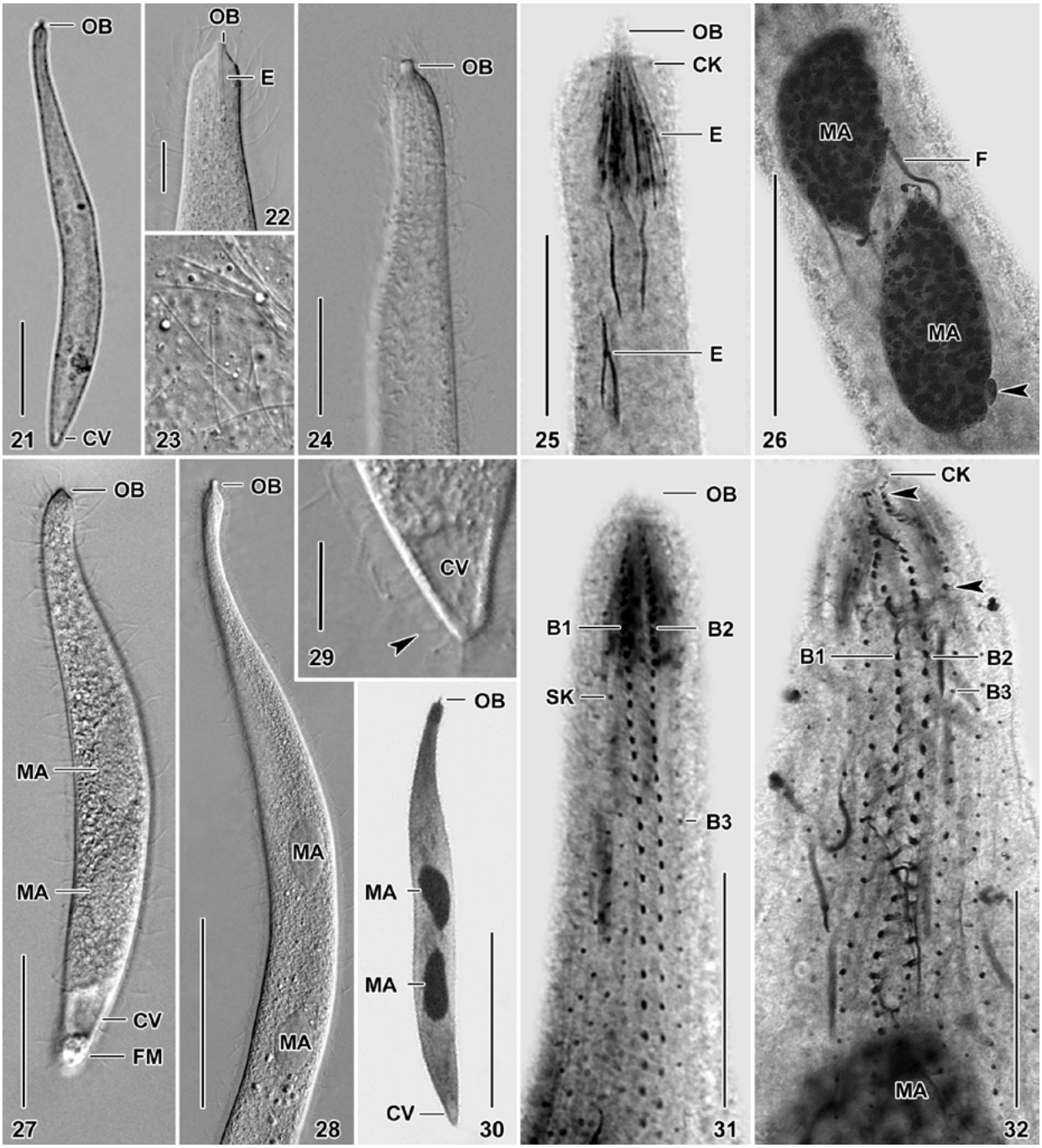

Figs 21–32. *Trachelophyllum brachypharynx*, Korean specimens *in vivo* (21–24, 27–29) and after protargol impregnation (25, 26, 30–32). **21, 27, 28, 30** – overview showing the narrowly fusiform body, the nuclear apparatus composed of two macronuclear nodules, and the turbid cytoplasm packed with many small granules and some lipid droplets; **22, 24, 25** – detail of the anterior body end showing the pin-shaped to conical oral bulge studded with extrusomes; **23** – extrusomes are about 30 µm long in vivo and are filiform with pointed and slightly curved ends; **26** – the nuclear apparatus is typically composed of two ellipsoidal macronuclear nodules that are distinctly separate and connected by a fine strand. The arrowhead denotes an ellipsoidal micronucleus; **29** – detail of the rear body end showing the single posterior contractile vacuole and hat-shaped lepidosomes (arrowhead) forming a mucilaginous layer around the cell; **31** – dorsal view of the ciliary pattern in the anterior body portion of a typical specimen. The dorsal brush is composed of two isostichad dikinetidal rows and a single monokinetidal row; **32** – dorsal view of the ciliary pattern in the anterior body portion of a malformed specimen whose brush row 3 also commences with a dikinetidal part (arrowheads) similar to the first two brush rows. B1–3 – dorsal brush row 1–3, CK – circumoral kinety, CV – contractile vacuole, E – extrusomes, F – fiber, FM – fecal mass, MA – macronuclear nodules, OB – oral bulge, SK – somatic kinety. Scale bars: 10 µm (29), 30 µm (22, 26, 31, 32), 50 µm (24, 25), and 100 µm (21, 27, 28, 30).

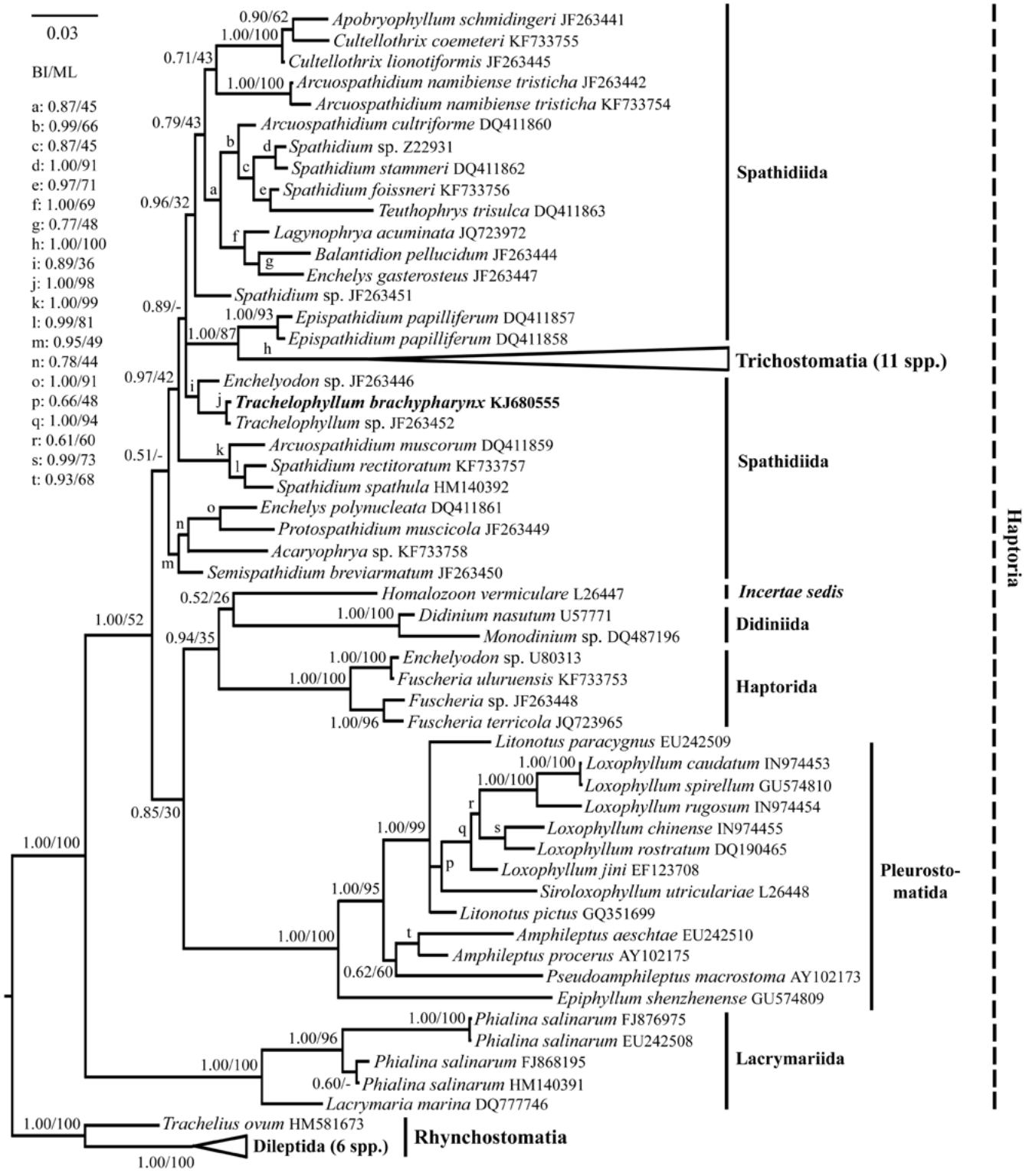

Fig. 33. Bayesian inference (BI) tree inferred from 1476 nucleotide characters of 69 litostomatean taxa under the GTR + I (= 0.5960) + Γ (= 0.4870) evolutionary substitution model. Results from maximum likelihood (ML) bootstrap analysis are mapped onto the Bayesian phylogenetic tree. A dash indicates a mismatch in the branching pattern. The scale bar indicates three substitutions per 100 nucleotide positions.

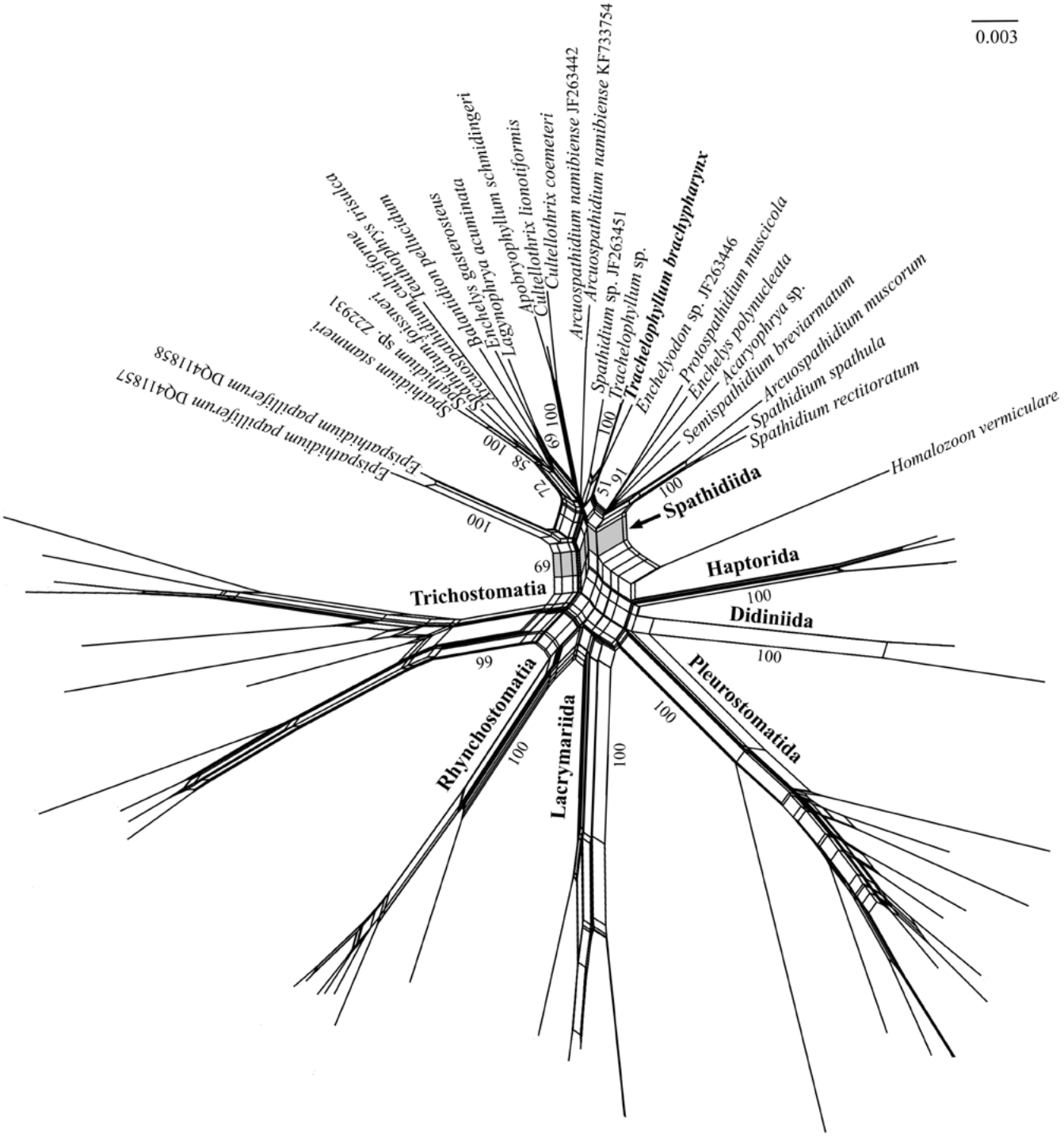

Fig. 34. Phylogenetic network inferred from 1,476 nucleotide characters of 69 litostomatean taxa, using the NeighborNet algorithm and the uncorrected distances. Numbers along the edges indicate bootstrap support values coming from 1,000 replicates. Only bootstraps > 50% and relevant to this study are shown. The scale bar indicates three substitutions per one thousand nucleotide positions.

tests ($p < 0.05$), but not by the WSH test ($p = 0.051$; Table 1). A monophyletic origin of spathidiids and haptorids with this pattern was statistically firmly excluded by all tree topology tests ($p < 0.001$). This indicates that the enchelyodonid cytoarchitecture evolved independently between the haptorids and spathidiids. Further, this ciliary organization very likely formed at least two times convergently within the spathidiids, once in the *Enchelyodon*-trachelophyllid lineage and a second time in the genus *Lagynophrya*. On the other hand, a sister relationship of the trachelophyllids and *Spathidium* sp. JF263451, as indicated in the phylogenetic networks, was not rejected by any statistical test ($p > 0.05$). This corroborates a relatively close phylogenetic relationship between the spathidiids *sensu stricto* and trachelophyllids.

DISCUSSION

Comparison of Korean population with original description

Levander's (1894) original description of *Trachelophyllum brachypharynx* is rather incomplete and confusing. Specifically, the nuclear apparatus was described as follows: "Three (two?) big, globular, homogenously appearing macronuclei in the mid-body". Concerning the contractile vacuole pattern, Levander (1894) wrote: "In the rear end of the body, there is a big, contractile vacuole that empties through a postero-terminal opening. I saw a bright big vacuole in the depicted specimen also at the transition between neck and body, but am not sure whether it was contractile as well". The length and shape of the extrusomes were not provided, but they were depicted as comparatively long and fine rods. Likewise, the mucilaginous cell cover was not reported (Figs 35 and 36) and no redescription of this species is available. Under these circumstances, it is not possible to unambiguously identify any population as *T. brachypharynx.* In spite of this, the Korean population described here matches Levander's (1894) specimens in body shape and size (330–445 μm vs. 350–400 μm) as well as in body flattening. Moreover, both populations were found in salt water: Levander (1894) discovered *T. brachypharynx* at the Finnish Gulf coast near the town of Helsinki while we found it in brackish water from the mouth of the Taehwa River as it opens into the East Sea, near the surrounding town of Ulsan, South Korea. Since this is the only trachelophyllid species reported from brackish and marine environments (e.g., Coats and Clamp 2009; Levander 1894, 1901; Telesh *et al.* 2009) and the body shape and size matches, we considered the Korean population to be conspecific with *T. brachypharynx*. Since 18S rRNA gene sequence is available for the Korean population, its conspecificity with *T. brachypharynx* can be also tested in the future by comparison with sequences from other saltwater populations, especially with those from the Finnish coast. To avoid nomenclatural and taxonomical problems, we decided to not designate the Korean population as the neotype of this species.

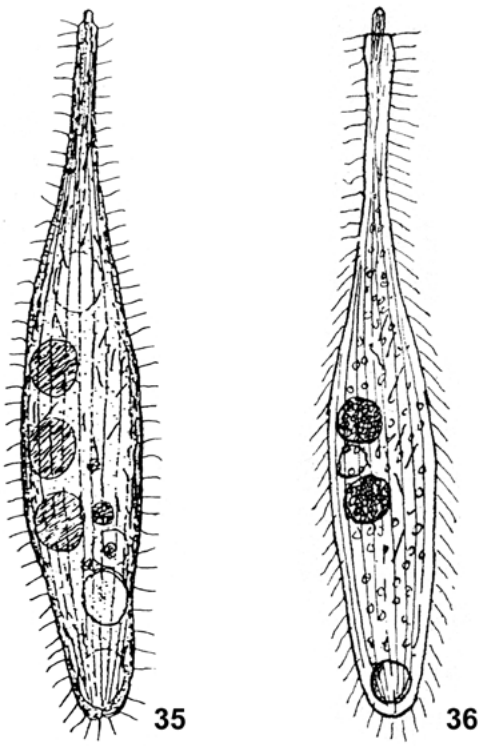

Fig. 35. Original drawing of *Trachelophyllum brachypharynx*, length 350–400 μm (from Levander 1894). **Fig. 36.** Redrawing of *T. brachypharynx*, length 400 μm (from Kahl 1930).

Generic home and comparison with similar species

Generic classification of trachelophyllids is based on the shape of lepidosomes (Foissner 1994, 2005; Foissner *et al.* 2002). The Korean population of *T. brachypharynx* exhibited hat-shaped lepidosomes whose presence is the key feature of the genus *Sleighophrys* (Foissner 2005). Unfortunately, there was not enough material to conduct SEM investigations on lepidosomes of the Korean *T. brachypharynx* population. Therefore, we can-

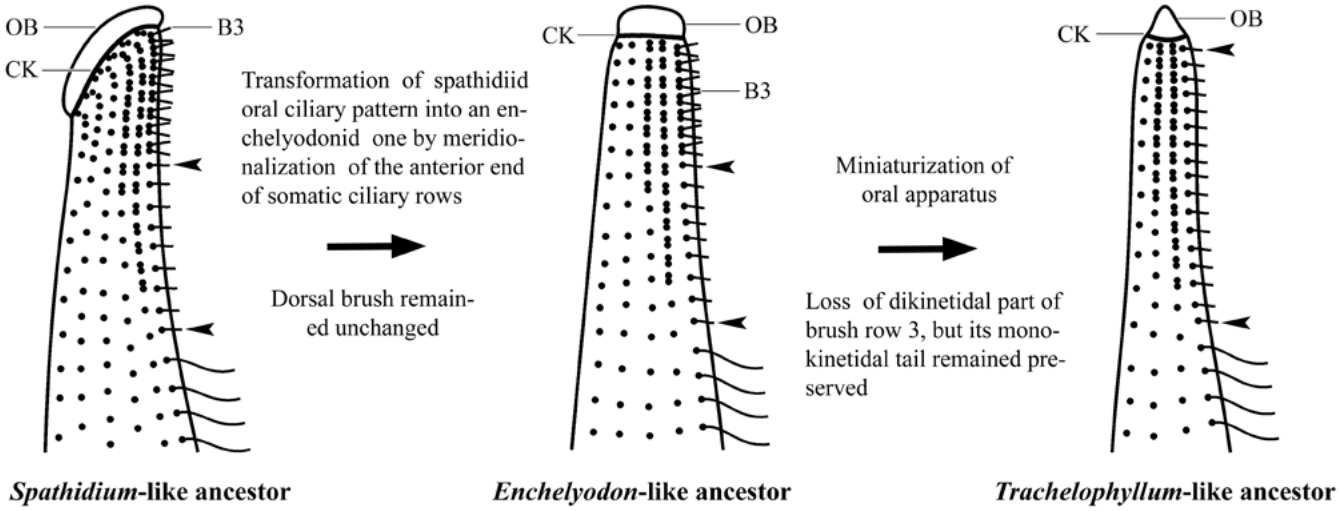

Fig. 37. Hypothesis for the morphological evolution of trachelophyllids from a *Spathidium*-like ancestor via an *Enchelyodon*-like stage. Arrowheads mark the monokinetidal tail of brush row 3. B3 – dorsal brush row 3, CK – circumoral kinety, OB – oral bulge.

not exclude that there are also other lepidosome types scattered between the hat-shaped type. Further research might very likely show that *T. brachypharynx* belongs to the genus *Sleighophrys*. But due to the lack of detailed SEM observations on lepidosomes, we prefer to not make any new combinations and maintain the original affiliation of *brachypharynx* with *Trachelophyllum.*

Besides *T. brachypharynx*, there are only two trachelophyllids with hat-shaped extrusomes, viz., *Trachelophyllum sigmoides* Kahl, 1926 and *S. pustulata* Foissner, 2005. While the lepidosomes of *T. sigmoides* were not described by Kahl (1926, 1930), Foissner (2005) noted that they are "mushroom-shaped and about 3.5 µm in size". The less studied *T. sigmoides* resembles *T. brachypharynx* in body size (250–400 µm vs. 330–445 µm), the nuclear and contractile vacuole apparatus (two separated macronuclear nodules each with a micronucleus and a single terminal vacuole) as well as in the extrusome pattern (one type of long filiform extrusomes). However, both species can be differentiated by body shape. Specifically, *T. sigmoides* is asymmetric with the anterior body portion distinctly curved to one side, causing the other to become sigmoidal (Kahl 1926, 1930). On the other hand, *T. brachypharynx* does not assume such a pattern and has an ordinary trachelophyllid shape (Levander 1894; present study). Further, *T. sigmoides* lives in saprobe puddles while *T. brachypharynx* resides in brackish and marine habitats.

Sleighophrys pustulata is distinguished from *T. brachypharynx* by a smaller body (160–230 µm vs. 330–445 µm), a lower number of ciliary rows (11–13 vs. 20–25), and a different extrusome pattern. Namely, *S. pustulata* exhibits two extrusome shape and size types: type I is acicular and 12–16 µm long, while type II is rod-shaped and only 2.5 µm long (Foissner 2005). On the other hand, *T. brachypharynx* displays only one type of about 30 µm long filiform extrusomes. Interestingly, *S. pustulata* was found in a slightly saline (4‰) sample that was taken from small flat depressions in the surroundings of the Flamingo lakes in Venezuela and consisted of dry cyanobacterial and algal crust, mud with plant litter, and loamy soil (Foissner 2005). On the other hand, *T. brachypharynx* is a true inhabitant of brackish and marine habitats (e.g., Coats and Clamp 2009; Levander 1894, 1901; Telesh *et al.* 2009; present study).

Phylogeny of trachelophyllids

Recent molecular studies have indicated that trachelophyllids belong to the order Spathidiida, a taxonomically and phylogenetically difficult assemblage of free-living litostomateans (Vďačný *et al.* 2011, 2012, 2014; Vďačný and Foissner 2013). However, about 20 years ago, Grain (1994) classified trachelophyllids at the suborder level within the Spathidiida. Foissner *et al.* (2002) followed and supported Grain's classification by

distinct similarities in the spathidiid and trachelophyllid oral and somatic ciliary pattern, especially in the structure of the dorsal brush and its monokinetidal tail associated with row 3. Later, Foissner (2005) suggested a relationship between trachelophyllids and lacrymariids because bifurcated nematodesmata were found in *Luporinophrys micelae* Foissner, 2005. However, bifurcated nematodesmata occur also in other haptorians, for instance, in the acropisthinids (Lipscomb and Riordan 1990; Foissner 2005), which also cluster within the Spathidiida in molecular phylogenies (Vďačný *et al.* 2011, 2012, 2014). Nevertheless, the structure and origin of nematodesmata are not appropriate features to determine haptorian phylogenetic relationships because of their highly homoplastic nature (Vďačný *et al.* 2011). On the other hand, dorsal brush features are more appropriate for these purposes, as recently documented by Kwon *et al.* (2014).

Trachelophyllids represent a distinct lineage within the Spathidiida as they significantly deviate from typical spathidiids in that (i) their body is contractile, fusiform, and covered by a mucilaginous layer of complex organic epicortical scales; (ii) their oral ciliature is in an enchelyodonid pattern, whereby the anterior end of the somatic kineties is not curved in the oral region; and (iii) only the first two brush rows are dikinetidal while the third row is monokinetidal throughout (Foissner 1994, 2005; Foissner *et al.* 1999, 2002). On the other hand, typical spathidiids (i) lack lepidosomes; (ii) their oral ciliature forms a spathidiid pattern in that the anterior end of the ciliary rows is curved rightward; and (iii) all three brush rows are made of dikinetids, with only the third row continuing as a monokinetidal tail (Foissner and Xu 2007). These discrepancies between trachelophyllid and spathidiid morphologies can be reconciled in the light of the present phylogenetic analyses that indicate members of the genera *Spathidium* and *Enchelyodon* as the nearest relatives of trachelophyllids. Specifically, phylogenetic trees consistently showed a sister relationship between *Enchelyodon* sp. JF263446 and trachelophyllids (Fig. 33), while phylogenetic networks suggested *Spathidium* sp. JF263451 as the nearest relative of trachelophyllids (Fig. 34). Based on these facts and looking at the morphology of *Spathidium*, *Enchelyodon,* and *Trachelophyllum*, we hypothesize that the spathidiid oral ciliary pattern transformed into an enchelyodonid pattern by meridionalization of the anterior end of somatic ciliary rows. However, the dorsal brush remained unchanged at this stage, meaning all three brush rows were dikinetidal and row 3 continued posteriorly with a monokinetidal tail (Vďačný and Foissner 2013). This morphological grade was virtually maintained in *Enchelyodon*. In the next evolutionary step, (i) the body became covered by epicortical scales; (ii) the oral apparatus miniaturized, which resulted in the formation of a conical oral bulge; and (iii) the dikinetidal part of brush row 3 was lost, leaving only the monokinetidal tail (Fig. 37). However, we found a single malformed specimen whose brush row 3 began with a short dikinetidal portion (Figs 7 and 32). We consider this morphological deviation to be reminiscent of the *Enchelyodon*-like stage present in the evolutionary history of trachelophyllids, providing strong evidence corroborating our hypothesis. However, the matter is complex because according to the molecular and combined morphological-molecular phylogenies as well as the statistical tree topology tests, the *Enchelyodon*-like body organization evolved convergently several times within the subclass Haptoria (Vďačný and Foissner 2013; present study); once in the order Haptorida and at least two times independently in the order Spathidiida, viz., in the *Enchelyodon-Trachelophyllum* lineage and in the genus *Lagynophrya*. However, the available molecular data from trachelophyllids clearly show that their peculiar morphology originated only once within the order Spathidiida.

Acknowledgements. We are indebted to Dr. William A. Bourland for his help with obtaining the Levander (1894) study. Technical assistance of Dr. Marek Vďačný and MSc. Ji Hye Kim is greatly acknowledged. This study was supported by the grants provided by the National Research Foundation of Korea (Project No. 2012R1A1A2005751), the National Institute of Biological Resources (NIBR) of the Ministry of Environment, Korea (project 1834-302), and the Slovak Scientific Grant Agency VEGA (Project No. 1/0248/13). This work was supported by the Slovak Research and Development Agency under the contract No. APVV-0436-12.

REFERENCES

Castresana J. (2000) Selection of conserved blocks from multiple alignments for their use in phylogenetic analysis. *Mol. Biol. Evol.* **17:** 540–552

Chen Z., Song W. (2001) Phylogenetic positions of *Uronychia transfuga* and *Diophrys appendiculata* (Euplotida, Hypotrichia, Ciliophora) within hypotrichous ciliates inferred from the small ribosomal RNA gene sequences. *Eur. J. Protistol.* **37:** 291–301

Coats D. W., Clamp J. C. (2009) Ciliated protists (Ciliophora) of the Gulf of Mexico. In: Gulf of Mexico: Origin, Waters, and Biota, Vol. 1. Biodiversity, (Eds. D. L. Felder, D. K. Camp). Texas A&M University Press, 57–79

Foissner W. (1984) Infraciliatur, Silberliniensystem und Biometrie einiger neuer und wenig bekannter terrestrischer, limnischer

und mariner Ciliaten (Protozoa: Ciliophora) aus den Klassen Kinetofragminophora, Colpodea und Polyhymenophora. *Stapfia* **12:** 1–165

Foissner W. (1994) *Spetazoon australiense* nov. gen., nov. spec., ein neues Wimpertier (Protozoa, Ciliophora) von Australien. *Kataloge des OÖ. Landesmuseums (N. F.)* **71:** 267–278

Foissner W. (2005) Two new "flagship" ciliates (Protozoa, Ciliophora) from Venezuela: *Sleighophrys pustulata* and *Luporinophrys micelae*. *Eur. J. Protistol*. **41:** 99–117

Foissner W., Xu K. (2007) Monograph of the Spathidiida (Ciliophora, Haptoria). Vol. I: Protospathidiidae, Arcuospathidiidae, Apertospathulidae. Springer-Verlag, Dordrecht

Foissner W., Berger H., Blatterer H., Kohmann F. (1995) Taxonomische und ökologische Revision der Ciliaten des Saprobiensystems – Band IV: Gymnostomatea, *Loxodes*, Suctoria. Informationsberichte des Bayerischen Landesamtes für Wasserwirtschaft, Deggendorf

Foissner W., Berger H., Schaumburg J. (1999) Identification and ecology of limnetic plankton ciliates. Informationsberichte des Bayerischen Landesamtes für Wasserwirtschaft, Deggendorf

Foissner W., Agatha S., Berger H. (2002) Soil ciliates (Protozoa, Ciliophora) from Namibia (Southwest Africa) with emphasis on two contrasting environments, the Etosha region and the Namib Desert. *Denisia* **5:** 1–1459

Grain J. (1994) Classe de Litostomatea. In: Infusoires Ciliés–Systematique, Traité de Zoologie, Vol. II, Fasc. 2, (Ed. P. de Puytorac). Masson, Paris, 267–310

Guindon S., Gascuel O. (2003) A simple, fast, and accurate algorithm to estimate large phylogenies by maximum likelihood. *Syst. Biol.* **52:** 696–704

Guindon S., Dufayard J. F., Lefort V., Anisimova M., Hordijk W., Gascuel O. (2010) New algorithms and methods to estimate maximum-likelihood phylogenies: assessing the performance of PhyML 3.0. *Syst. Biol.* **59:** 307–321

Huson D. H. (1998) SplitsTree: a program for analyzing and visualizing evolutionary data. *Bioinformatics* **14:** 68–73

Huson D. H., Bryant D. (2006) Application of phylogenetic networks in evolutionary studies. *Mol. Biol. Evol.* **23:** 254–267

International Commission on Zoological Nomenclature [ICZN] (1999) International Code of Zoological Nomenclature. 4th ed. Tipografia La Garangola, Padova

Kahl A. (1926) Neue und wenig bekannte Formen der holotrichen und heterotrichen Ciliaten. *Arch. Protistenkd.* **55:** 197–438

Kahl A. (1930) Urtiere oder Protozoa I: Wimpertiere oder Ciliata (Infusoria) 1. Allgemeiner Teil und Prostomata. *Tierwelt Dtl.* **18:** 1–180

Katoh K., Toh H. (2008) Recent developments in the MAFFT multiple sequence alignment program. *Brief. Bioinform.* **9:** 286–298

Kwon C. B., Vďačný P., Shazib S. U. A., Shin M. K. (2014) Morphology and molecular phylogeny of a new haptorian ciliate, *Chaenea mirabilis* sp. n., with implications for the evolution of the dorsal brush in haptorians (Ciliophora, Litostomatea). *J. Eukaryot. Microbiol.* **61:** 278–292

Levander K. M. (1894) Materialien zur Kenntnis der Wasserfauna in der Umgebung von Helsingfors, mit besonderer Berücksichtigung der Meeresfauna. I. Protozoa. *Acta Soc. Fauna Flora fenn.* **12:** 1–115

Levander K. M. (1901) Übersicht der in der Umgebung von Esbo-Löfö im Meereswasser vorkommenden Thiere. *Acta Soc. Fauna Flora fenn.* **20:** 1–20

Lipscomb D. L., Riordan G. P. (1990) The ultrastructure of *Chaenea teres* and an analysis of the phylogeny of the haptorid ciliates. *J. Protozool.* **37:** 287–300

Medlin L., Elwood H. J., Stickel S., Sogin M. L. (1988) The characterization of enzymatically amplified eukaryotic 16S-like rRNA-coding regions. *Gene* **71:** 491–499

Posada D. (2008) JModelTest: phylogenetic model averaging. *Mol. Biol. Evol.* **25:** 1253–1256

Ronquist F., Huelsenbeck J. P. (2003) MrBayes 3: Bayesian phylogenetic inference under mixed models. *Bioinformatics* **19:** 1572–1574

Shimodaira H. (2002) An approximately unbiased test of phylogenetic tree selection. *Syst. Biol.* **51:** 492–508

Shimodaira H. (2008) Testing regions with non-smooth boundaries via multiscale bootstrap. *J. Stat. Plan. Infer.* **138:** 1227–1241

Shimodaira H., Hasegawa M. (2001) Consel: for assessing the confidence of phylogenetic tree selection. *Bioinformatics* **17:** 1246–1247

Swofford D. L. (2003) PAUP*. Phylogenetic Analysis Using Parsimony (*and Other Methods). Ver. 4. Sinauer Associates, Sunderland, MA

Talavera G., Castresana J. (2007) Improvement of phylogenies after removing divergent and ambiguously aligned blocks from protein sequence alignments. *Syst. Biol.* **56:** 564–577

Telesh I., Postel L., Heerkloss R., Mironova E., Skarlato S. (2009) Zooplankton of the open Baltic Sea: extended atlas. *Meereswiss. Ber., Warnemünde* **76:** 1–290

Vďačný P., Foissner W. (2013) Synergistic effects of combining morphological and molecular data in resolving the phylogenetic position of *Semispathidium* (Ciliophora, Haptoria), with description of *S. breviarmatum* sp. n. from tropical Africa. *Zool. Scr.* **42:** 529–549

Vďačný P., Bourland W. A., Orsi W., Epstein S. S., Foissner W. (2011) Phylogeny and classification of the Litostomatea (Protista, Ciliophora), with emphasis on free-living taxa and the 18S rRNA gene. *Mol. Phylogenet. Evol.* **59:** 510–522

Vďačný P., Bourland W. A., Orsi W., Epstein S. S., Foissner W. (2012) Genealogical analyses of multiple loci of litostomatean ciliates (Protista, Ciliophora, Litostomatea). *Mol. Phylogenet. Evol.* **65:** 397–411

Vďačný P., Breiner H.-W., Yashchenko V., Dunthorn M., Stoeck T., Foissner W. (2014) The chaos prevails: molecular phylogeny of the Haptoria (Ciliophora, Litostomatea). *Protist* **165:** 93–111

Wilbert N. (1975) Eine verbesserte Technik der Protargolimprägnation für Ciliaten. *Mikrokosmos* **64:** 171–179

Received on 23rd April, 2014; revised on 19th August, 2014; accepted on 16th September, 2014